DOI: 10.1534/genetics.108.088427

Bayesian Quantitative Trait Loci Mapping for Multiple Traits

Samprit Banerjee,* Brian S. Yandell† and Nengjun Yi*,[1]

**Department of Biostatistics, Section on Statistical Genetics, University of Alabama, Birmingham, Alabama 35294 and* †*Departments of Statistics, Horticulture and Biostatistics and Medical Informatics, University of Wisconsin, Madison, Wisconsin 53706*

Manuscript received February 22, 2008
Accepted for publication June 15, 2008

ABSTRACT

Most quantitative trait loci (QTL) mapping experiments typically collect phenotypic data on multiple correlated complex traits. However, there is a lack of a comprehensive genomewide mapping strategy for correlated traits in the literature. We develop Bayesian multiple-QTL mapping methods for correlated continuous traits using two multivariate models: one that assumes the same genetic model for all traits, the traditional multivariate model, and the other known as the seemingly unrelated regression (SUR) model that allows different genetic models for different traits. We develop computationally efficient Markov chain Monte Carlo (MCMC) algorithms for performing joint analysis. We conduct extensive simulation studies to assess the performance of the proposed methods and to compare with the conventional single-trait model. Our methods have been implemented in the freely available package R/qtlbim (http://www.qtlbim.org), which greatly facilitates the general usage of the Bayesian methodology for unraveling the genetic architecture of complex traits.

COMPLEX traits involve effects of a multitude of genes in an interacting network. Mapping quantitative trait loci (QTL) means inferring the genetic architecture (number of genes, their positions, and their effects) underlying these complex traits. The QTL mapping problem has several salient features: first, the predictor variables in the regression (the genotypes of QTL) are not observed; second, it is really a model selection problem as there are typically thousands of loci to choose from; and third, the genomic loci on the same chromosome are correlated. Much has been done in this regard, especially in the univariate case (*e.g.*, Lander and Botstein 1989; Jiang and Zeng 1997; Broman and Speed 2002). Bayesian methods have been very successful in the QTL mapping framework (Satagopan and Yandell 1996; Yi and Xu 2002; Yi *et al.* 2003, 2005, 2007; Yi 2004); see a recent review by Yi and Shriner (2008).

Most of these methods are applicable to mapping QTL for a single trait. However, in QTL experiments typically data on more than one trait are collected and, more often than not, they are correlated. It seems natural to jointly analyze these correlated traits. There are two distinct advantages for jointly analyzing correlated traits: including information from all traits can increase the power to detect QTL and the precision of the estimated QTL effects. Biologically, it is imperative to jointly analyze correlated traits to answer questions like pleiotropy (one gene influencing more than one trait) and/or close linkage (different QTL physically close to each other influencing the traits). Testing these hypotheses is key to understanding the underlying biochemical pathways causing complex traits, which is the ultimate goal of QTL mapping.

Several methods have been developed to jointly analyze multiple correlated traits. Some of them use a maximum-likelihood-based approach (Jiang and Zeng 1995; Jackson *et al.* 1999; Williams *et al.* 1999a,b; Vieira *et al.* 2000; Huang and Jiang 2003; Lund *et al.* 2003; Xu *et al.* 2005) or a least-squares approach (Knott and Haley 2000; Hackett *et al.* 2001). Most of these methods involve a single-QTL model or at most very few QTL. A problem with the likelihood-based approach is that with increasing complexity, due to the increase in the number of parameters to be estimated, the increase in degrees of freedom of the test statistic can restrain its practical use when the number of traits is large (Mangin *et al.* 1998). As a result, the advantage of joint analysis is lost over single-trait analysis. Another approach for joint analysis is to use a dimension reduction technique, namely, principal component analysis (PCA) or discriminant analysis (DA) or using canonical variables associated with the traits (Mangin *et al.* 1998; Mähler *et al.* 2002; Gilbert and Le Roy 2003, 2004), and then use the linear combination of traits to map QTL. The problem with this approach is that linear combinations of traits are not biologically interpretable and can cause spurious linkages (Mähler *et al.* 2002; Gilbert and Le Roy 2003). Gilbert and Le Roy (2003) compared the performance of PCA, DA, and the multivariate model in a full-sib family and half-sib families under differ-

[1]*Corresponding author:* Department of Biostatistics, University of Alabama, Birmingham, AL 35294-0022. E-mail: nyi@ms.soph.uab.edu

ent scenarios. Lange and Whittaker (2001) use a nonparametric generalized estimating equations approach to multivariate QTL mapping.

Meuwissen and Goddard (2004) used a Markov chain Monte Carlo (MCMC) algorithm to map QTL, using linkage disequilibrium and linkage information for multiple-traits data. Recently, Liu *et al.* (2007) developed a Bayesian approach to map QTL for a combination of normal and ordinal traits in a full-sib design based on the variance components approach. They used a reversible-jump (RJ) MCMC to estimate the unknown number of QTL. The problem with RJ-MCMC is that increased complexity drastically increases the computational burden, rendering it unsuitable for genomewide scans where typically thousands of positions are scanned for a putative QTL. Another major challenge is to ascertain convergence of the RJ sampler and obtain a rapidly converging sampler (Yi 2004). Yang and Xu (2007) extended the Bayesian shrinkage analysis with a fixed-interval approach (Wang *et al.* 2005), where a QTL is placed in each marker interval, to a moving-interval approach, where the position of a QTL can be searched in a range that covers many marker intervals for dynamic/longitudinal traits using a Legendre polynomial. Their method, however, focuses on the study of the growth trajectory of time-dependent or repeated-measures types of outcomes (called dynamic traits) and is very different from our approach.

All the multivariate methods mentioned here use the traditional multivariate regression model, which assumes the same genetic model for all traits. However, almost all correlated traits are actually affected to some extent by a different multilocus network. To capture this facet of multiple traits we use the so-called "seemingly unrelated regression" (SUR) model (Zellner 1962), which allows each trait to have a different set of QTL. Verzilli *et al.* (2005) implemented a Bayesian version of SUR using RJ-MCMC to jointly analyze multiple correlated traits with SNP data in a human population. They found it difficult "to deal with very many loci" and restricted attention to only 12 SNPs. Their method appears unsuitable to genomewide scans.

In the literature of joint analysis for QTL mapping, there is a lack of comprehensive genomewide strategies to map multiple pleiotropic and nonpleiotropic QTL. In this article, we extend the composite model space approach of Yi (2004) to jointly analyze multiple correlated continuous traits. Multiple traits are modeled using novel QTL SUR models that enable us to detect either the same or different QTL for different traits, facilitating the separation of pleiotropy and close linkage. The QTL SUR models include the traditional multivariate model and the single trait-by-trait model as special cases. We develop computationally efficient MCMC algorithms for performing joint analysis. Finally, we conduct extensive simulation studies to assess the performance of the proposed methods.

BAYESIAN MODELING OF MULTIPLE QTL FOR MULTIPLE TRAITS

QTL SUR models: We focus our attention on experimental crosses derived from two inbred lines. Observed data in QTL mapping consist of phenotypic values of complex traits and molecular marker data. We extend the composite model space approach of Yi (2004) to jointly analyze multiple correlated continuous traits. We assume that the marker data include not only the marker genotypes but also the genomic positions of the markers. We approximate positions for all possible QTL using a partition of the entire genome into evenly spaced loci, including all observed markers and additional loci (called pseudomarkers) between flanking markers (Sen and Churchill 2001; Yi *et al.* 2005). Inserting pseudomarkers enables us to detect potential QTL within the marker intervals, but introduces a special statistical problem; *i.e.*, QTL genotypes are unobserved. Before mapping QTL, we calculate the probabilities of genotypes at these preset loci given the observed marker data as priors of QTL genotypes in our Bayesian framework.

The actual number of detectable QTL for each trait in a particular experiment is unknown, but usually not too large. We employ a composite model space approach (Yi 2004; Yi *et al.* 2005) and consider at most L possible loci. The upper bound L is larger than the number of detectable QTL with high probability for a given data set and can be set on the basis of the initial analyses using conventional mapping methods on each trait (Yi 2004; Yi *et al.* 2005). Conditioning on the genotypes at these L loci for all individuals, the phenotypic values y_{ti} for individual i on trait t can be expressed as a linear regression,

$$y_{ti} = \mu_t + \mathbf{X}_{ti}\boldsymbol{\beta}_t + e_{ti}, \quad t = 1, 2, \cdots, T, \quad i = 1, 2, \cdots, n, \tag{1}$$

where T and n represent the numbers of traits and individuals, respectively, the subscripts t and i represent the tth trait and the ith individual, respectively, μ_t is the overall mean for trait t, $\mathbf{X}_{ti}$ is the row vector of the main-effect predictors of L loci, determined from the genotypes by using a particular genetic model [we use the Cockerham genetic model, although other genetic models are possible (Kao and Zeng 2002; Zeng *et al.* 2005)], $\boldsymbol{\beta}_t$ is the vector of all main effects for L loci of trait t, and the vector of residual errors across traits, $\mathbf{e}_i$, is independent and normal with mean $\mathbf{0}$ and covariance matrix $\boldsymbol{\Sigma}$; *i.e.*, $\mathbf{e}_i \sim N_T(\mathbf{0}, \boldsymbol{\Sigma})$. Thus, the residual errors are independent among individuals, but are correlated among traits within individuals. The above equations can be rewritten as

$$\mathbf{y}_i \sim N_T(\boldsymbol{\mu} + \mathbf{X}_i\boldsymbol{\beta}, \boldsymbol{\Sigma}), \quad i = 1, 2, \cdots, n, \tag{2}$$

where $\mathbf{y}_i = (y_{1i}, \cdots, y_{Ti})'$, $\boldsymbol{\mu} = (\mu_1, \cdots, \mu_T)'$, $\mathbf{X}_i = \mathrm{diag}(\mathbf{X}_{1i}, \cdots, \mathbf{X}_{Ti})$, and $\boldsymbol{\beta} = (\boldsymbol{\beta}_1', \cdots, \boldsymbol{\beta}_T')'$. This model

can include a large number of effects, many of which are irrelevant to modeling the phenotype and should be excluded from the model. We use an unobserved vector of indictor variables $\boldsymbol{\gamma}_t = (\gamma_{t1}, \gamma_{t2}, \cdots, \gamma_{tj}, \cdots)$ to indicate which effects $\boldsymbol{\beta}_t = (\beta_{t1}, \beta_{t2}, \cdots, \beta_{tj}, \cdots)'$ are included in ($\gamma_{tj} = 1$) or excluded from ($\gamma_{tj} = 0$) the model for the tth trait. We denote the genomic positions of L loci for trait t by the vector $\boldsymbol{\lambda}_t = (\lambda_{t1}, \cdots, \lambda_{tL})$. The vector $(\boldsymbol{\lambda}_t, \boldsymbol{\gamma}_t)$ thus determines the genetic architecture of the tth trait, *i.e.*, the actual number of QTL, their positions, and the activity of the associated genetic effects. Our goal is to infer the posterior distribution of $(\boldsymbol{\lambda}_t, \boldsymbol{\gamma}_t)$ and estimate the associated genetic effects.

Model (1) or (2) uses trait-specific effect predictors ($\mathbf{X}_{ti}$), positions ($\boldsymbol{\lambda}_t$), and indicator variables ($\boldsymbol{\gamma}_t$), allowing each trait to have a different set of QTL or a different genetic model. Therefore, models for different traits seem unrelated, but actually are related through correlated residual errors (or observed phenotypes) or the genotypes of linked QTL. Hereafter, we refer the above model as the QTL SUR model. We consider two different SUR models. In the first model as described above, different traits can have different sets of L loci ($\boldsymbol{\lambda}_t$) and thus different indicator variables ($\boldsymbol{\gamma}_t$) and predictors ($\mathbf{X}_{ti}$). The second SUR model uses the same set of L loci, *i.e.*, $\boldsymbol{\lambda}_1 = \cdots = \boldsymbol{\lambda}_T \triangleq \boldsymbol{\lambda}$ and thus $\mathbf{X}_{1i} = \cdots = \mathbf{X}_{Ti}$, but different indicator variables for different traits. We denote these two SUR models by SUR modeling with different loci used for all traits (SURd) and SUR modeling with the same loci used for all traits (SURs). Note that both QTL SUR models include two existing models as special cases, the univariate single-trait approach (STA) where the residual errors are unrelated, *i.e.*, $\boldsymbol{\Sigma} = \mathbf{I}$, and the traditional multivariate (TMV) model where all traits have the same set of loci and the same indicator variables, *i.e.*, $\boldsymbol{\lambda}_1 = \cdots = \boldsymbol{\lambda}_T$, $\mathbf{X}_{1i} = \cdots = \mathbf{X}_{Ti}$, and $\boldsymbol{\gamma}_1 = \cdots = \boldsymbol{\gamma}_T$.

Prior distributions: To complete Bayesian modeling of QTL SUR, we need to specify prior distributions for all unknowns. We describe the prior distributions for the model SURd in detail (appendix a), which can be easily adapted to the models SURs and TMV. For SURd, unknowns include the positions $\boldsymbol{\lambda} = (\boldsymbol{\lambda}_1, \cdots, \boldsymbol{\lambda}_T)$, indicator variables $\boldsymbol{\gamma} = (\boldsymbol{\gamma}_1, \cdots, \boldsymbol{\gamma}_T)$, main effects $\boldsymbol{\beta}$, overall mean $\boldsymbol{\mu}$, residual covariance matrix $\boldsymbol{\Sigma}$, and genotypes $\mathbf{g} = (\mathbf{g}_{tiq};\ t = 1, \cdots, T;\ i = 1, \cdots, n;\ q = 1, \cdots, L)$, where $\mathbf{g}_{tiq}$ is the genotype of individual i for trait t at locus q.

As described in the previous section, the prior on $\mathbf{g}_{tiq}$ is the probability of the genotype given the observed marker data. For computational reasons, we directly work on the inverse matrix $\boldsymbol{\Sigma}^{-1}$ instead of $\boldsymbol{\Sigma}$ (see the next section and appendix b). The prior for $\boldsymbol{\Sigma}^{-1}$ can be taken to be the commonly used noninformative prior; *i.e.*, $p(\boldsymbol{\Sigma}^{-1}) \sim |\boldsymbol{\Sigma}^{-1}|^{-(1+T)/2}$ (see Gelman *et al.* 2004). We assume that the unknowns $(\boldsymbol{\lambda}_t, \boldsymbol{\gamma}_t, \mu_t, \boldsymbol{\beta}_t)$ are independent among the traits. For each trait, the priors on $(\boldsymbol{\lambda}_t, \boldsymbol{\gamma}_t, \mu_t, \boldsymbol{\beta}_t)$ can be specified as in Yi *et al.* (2005, 2007), which we describe in appendix a.

MARKOV CHAIN MONTE CARLO ALGORITHM

We fit the models using the MCMC algorithm, applied to the joint posterior density of all the unknowns $(\boldsymbol{\mu}, \boldsymbol{\beta}, \boldsymbol{\sigma}, \boldsymbol{\Sigma}^{-1}, \mathbf{g}, \boldsymbol{\lambda}, \boldsymbol{\gamma})$. The joint posterior distribution can be expressed as

$$p(\boldsymbol{\mu}, \boldsymbol{\beta}, \boldsymbol{\sigma}, \boldsymbol{\Sigma}^{-1}, \mathbf{g}, \boldsymbol{\lambda}, \boldsymbol{\gamma} \mid \mathbf{y}) \propto \prod_{i=1}^{n} p(\mathbf{y}_i \mid \boldsymbol{\mu}, \boldsymbol{\beta}, \boldsymbol{\Sigma}^{-1}, \mathbf{X}_i, \boldsymbol{\gamma}) \cdot p(\mathbf{g}, \boldsymbol{\mu}, \boldsymbol{\beta}, \boldsymbol{\sigma}, \boldsymbol{\Sigma}^{-1}, \boldsymbol{\lambda}, \boldsymbol{\gamma}), \tag{3}$$

where the likelihood $p(\mathbf{y}_i \mid \boldsymbol{\mu}, \boldsymbol{\beta}, \boldsymbol{\Sigma}^{-1}, \mathbf{X}_i, \boldsymbol{\gamma})$ is defined by model (2), and the prior $p(\mathbf{g}, \boldsymbol{\mu}, \boldsymbol{\beta}, \boldsymbol{\sigma}, \boldsymbol{\Sigma}^{-1}, \boldsymbol{\lambda}, \boldsymbol{\gamma})$ is described in the last section and appendix a, and the augmentation with hyperparameters $\boldsymbol{\sigma}$ presents the prior variances for the effects $\boldsymbol{\beta}$ (Yi *et al.* 2007; see appendix a). For notational convenience, we suppress the dependence on the observed marker data here and afterward.

The joint posterior distribution can be simulated using the Gibbs sampler and Metropolis algorithm, alternately updating each unknown conditional on all other parameters and the observed data. We show all the conditional distributions in appendix b. Conditional updates of $\boldsymbol{\mu}$, $\boldsymbol{\beta}$, $\boldsymbol{\sigma}$, and $\boldsymbol{\Sigma}^{-1}$ are the same for the models SURd, SURs, and TMV. However, conditional updates of $\mathbf{g}$, $\boldsymbol{\lambda}$, and $\boldsymbol{\gamma}$ are illustrated only for the SURd model, which can be easily adapted to the SURs and TMV models (see appendix b). Below, we describe our algorithm, with more details on steps for unknowns where the method involves explicit extension for multiple correlated traits.

A commonly used updating scheme for the overall means and the coefficients is performed by updating jointly $\boldsymbol{\mu}$ and $\boldsymbol{\beta}$ for all traits (see Smith and Kohn 2000; Griffiths 2001; Verzilli *et al.* 2005). This scheme requires large matrix operations at each simulation iteration, resulting in prohibitive computational burden for genomewide multiple-QTL analysis. We have developed a pure Gibbs sampler to update one parameter at a time: for each t and j, we sample μ_t and β_{tj} from their conditional posterior distributions, respectively, which are normal distributions (see Equations B1 and B2 in appendix b). This one-at-a-time algorithm never requires matrix operations and is computationally very efficient. Note that if $\gamma_{tj} = 0$, we do not need to sample β_{tj}.

The variance parameters σ^2_{tk} are updated one at a time: for each t and k, the conditional posterior distribution of σ^2_{tk} is a scaled inverse χ^2-distribution and can be directly sampled (see Equation B3 in appendix b). For computational convenience, we work on the inverse matrix $\boldsymbol{\Sigma}^{-1}$ instead of $\boldsymbol{\Sigma}$ (see appendix b). The conditional posterior distribution of $\boldsymbol{\Sigma}^{-1}$ is a stan-

TABLE 1

True positions of six QTL, their effects, and heritabilities

	Q_1	Q_2	Q_3	Q_4	Q_5	Q_6
Chromosome	1	1	2	2	3	4
Position (cM)	22	55	22	65	65	45
y_1	0.8	0.6	0	0	0.8	0.6
y_2	0	0	−0.8	−0.6	0.8	0.6
y_1 (%)	8.8	4.9	0	0	8.8	4.9
y_2 (%)	0	0	9.3	5.2	9.3	5.2

dard Wishart distribution, and thus both the Gibbs sampler and the Metropolis algorithm can be applied to update $\mathbf{\Sigma}^{-1}$ (see Equations B4 and B5).

The genotypes are usually updated one at a time from the conditional posterior distributions. If locus q is included in the model and the genotype g_{tiq} is not observed, the conditional posterior distribution of g_{tiq} is a simple multinomial (or binomial) distribution and thus can be sampled directly (see Equation B6); otherwise, we do not need to sample g_{tiq}. The positions $\boldsymbol{\lambda}$ are also updated one at a time. As above, we need to update only those loci that are included in the current model. The conditional posterior distribution of $(\lambda_{tq}, \mathbf{g}_{tq})$ is not a standard distribution, and thus a Metropolis algorithm is needed to update $(\lambda_{tq}, \mathbf{g}_{tq})$ (see Equations B7 and B8 in APPENDIX B).

The indicator variables $\boldsymbol{\gamma}$ are also updated one at a time. The binary indicator variables γ_{tj} for the SUR models have independently binomial conditional posterior distributions (see Equations B9 and B12 in APPENDIX B). At each iteration, therefore, the Gibbs sampler can be used to generate each indicator from its conditional posterior. However, for the QTL SUR models, using the Gibbs samplers is computationally demanding because the SUR models contain T times the number of indicators as a single-trait model and most of the indicators are zero. To speed up the algorithm we extend the Metropolis–Hastings (MH) algorithm proposed by YI *et al.* (2007) to the QTL SUR models in a natural way (see Equation B11). This MH algorithm can be easily adapted to the TMV model.

SUMMARIZING AND INTERPRETING THE POSTERIOR SAMPLES

Assessing the convergence and mixing behavior of any MCMC algorithm is somewhat difficult to ascertain and it is intensified for a high-dimensional problem. Several methods have been developed so far; many are implemented in R/coda (PLUMMER *et al.* 2004), an R package providing an object-based infrastructure for analyzing output of MCMC simulations and performing convergence diagnostics.

The posterior samples generated by the above MCMC algorithm contain all available information about the unknowns in the QTL SUR and thus the genetic architecture of the multiple traits. The vector (λ_t, γ_t) determines the number of QTL, their positions, and the main effects of QTL, for the tth trait and hence identifies its genetic architecture. The posterior inclusion probability for each locus is estimated as its frequency in the posterior samples. The larger the effect size is for a locus, the more frequently the locus is sampled. Taking the prior probability into consideration, we use Bayes factors (BF) to show evidence for inclusion against exclusion of a locus. Bayes factors are calculated on the basis of the idea of model averaging. The Bayes factor of the jth locus for the tth trait can be represented as the ratio of the posterior to prior odds of selecting that particular locus. Model averaging accounts for model uncertainty and hence provides more robust inference compared to a single "best" model approach (RAFTERY *et al.* 1997; BALL 2001; SILLANPÄÄ and CORANDER 2002).

Since the information about correlation between multiple traits is taken into account, the proposed QTL SUR model is expected to increase the probability

TABLE 2

Average correct and incorrect QTL detected for traits y_1 (first row) and y_2 (second row)

	Correct				Extraneous			
$(n, \rho_{y_1 y_2})$	STA	TMV	SURs	SURd	STA	TMV	SURs	SURd
(100, 0.5)	0.65	0.8	0.67	0.64	0.7	1.34	0.45	0.65
	0.74	0.78	0.64	0.81	0.39	1.36	0.26	0.59
(100, 0.8)	0.34	1.01	1.02	0.97	0.24	1.85	0.75	0.54
	0.78	1.07	1.3	1.21	0.71	1.72	0.84	0.78
(200, 0.5)	1.69	2.13	2.12	1.78	1.06	2.53	0.78	1.02
	1.76	2.2	2.16	1.67	0.63	2.55	0.78	0.69
(200, 0.8)	1.51	2.6	2.56	2.24	0.63	2.92	0.73	0.72
	1.75	2.61	2.66	2.4	0.96	2.96	0.84	0.8
(500, 0.5)	3.54	3.72	3.76	3.66	1.01	3.1	0.83	1.22
	3.59	3.79	3.75	3.56	0.76	3.07	0.67	0.88
(500, 0.8)	3.55	3.81	3.78	3.67	1.1	3.14	1.03	1.01
	3.64	3.8	3.75	3.62	1.18	3.11	0.6	0.84

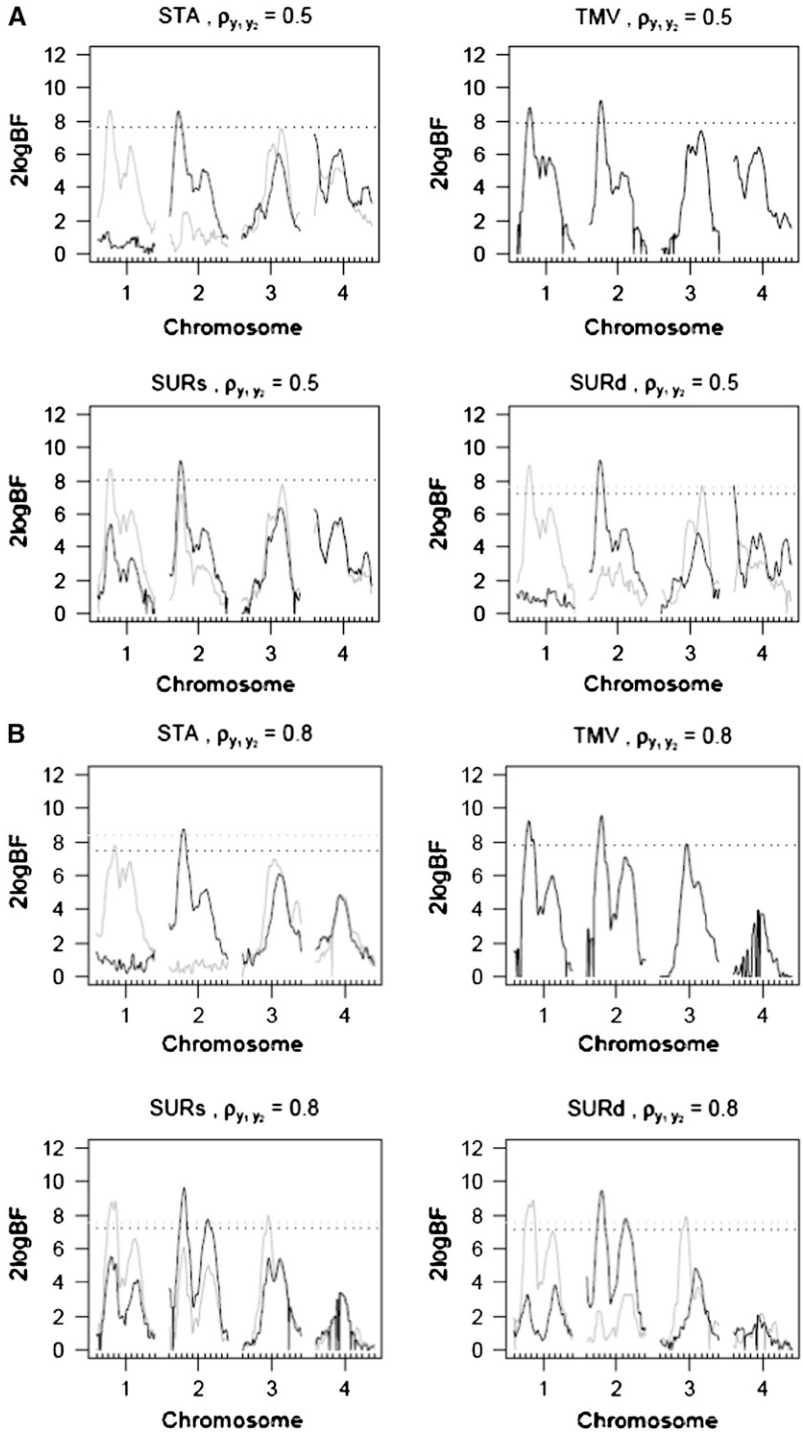

FIGURE 1.—(A) 2 logBF profile for $n = 100$ and $\rho_{y_1 y_2} = 0.5$ for all four methods. Shaded curves represent 2 logBF profile for y_1 and solid curves that for y_2; the shaded dotted lines denotes the 95% threshold for y_1 for the null model and the solid dotted lines denote the same for y_2. On the *x*-axis, large tick marks represent chromosomes and small tick marks represent markers. (B) 2 logBF profile for $n = 100$ and $\rho_{y_1 y_2} = 0.8$ for all four methods. Shaded curves represent 2 logBF profile for y_1 and solid curves that for y_2; shaded dotted lines denote the 95% threshold for y_1 for the null model and solid dotted lines denote the same for y_2. On the *x*-axis, large tick marks represent chromosomes and small tick marks represent markers.

of detecting QTL, especially weak-effect QTL. More importantly, the QTL SUR model allows for a statistically rigorous procedure to test a number of biologically important questions involving multiple traits, such as pleiotropy and pleiotropy *vs.* close linkage. To test if the *j*th locus is a pleiotropic QTL we considered all models that include the *j*th locus for all traits (*i.e.*, all models with $\gamma_{tj} = 1$ for all t) and compute the joint posterior inclusion probabilities. By jointly considering the positions $\boldsymbol{\lambda}$ and the indicators $\boldsymbol{\gamma}$, one can distinguish pleiotropy and close linkage.

IMPLEMENTATION IN R/QTLBIM

The proposed methods have been implemented in R/qtlbim (YANDELL *et al.* 2007), which is a freely available R library. The previous version of R/qtlbim performs only single-trait analysis. R/qtlbim is built on top of the widely used R/qtl (BROMAN *et al.* 2003) and provides an extensible, interactive environment for Bayesian analysis of multiple interacting QTL in experimental crosses. The MCMC algorithm is written in C and the graphics and data manipulation are performed in R.

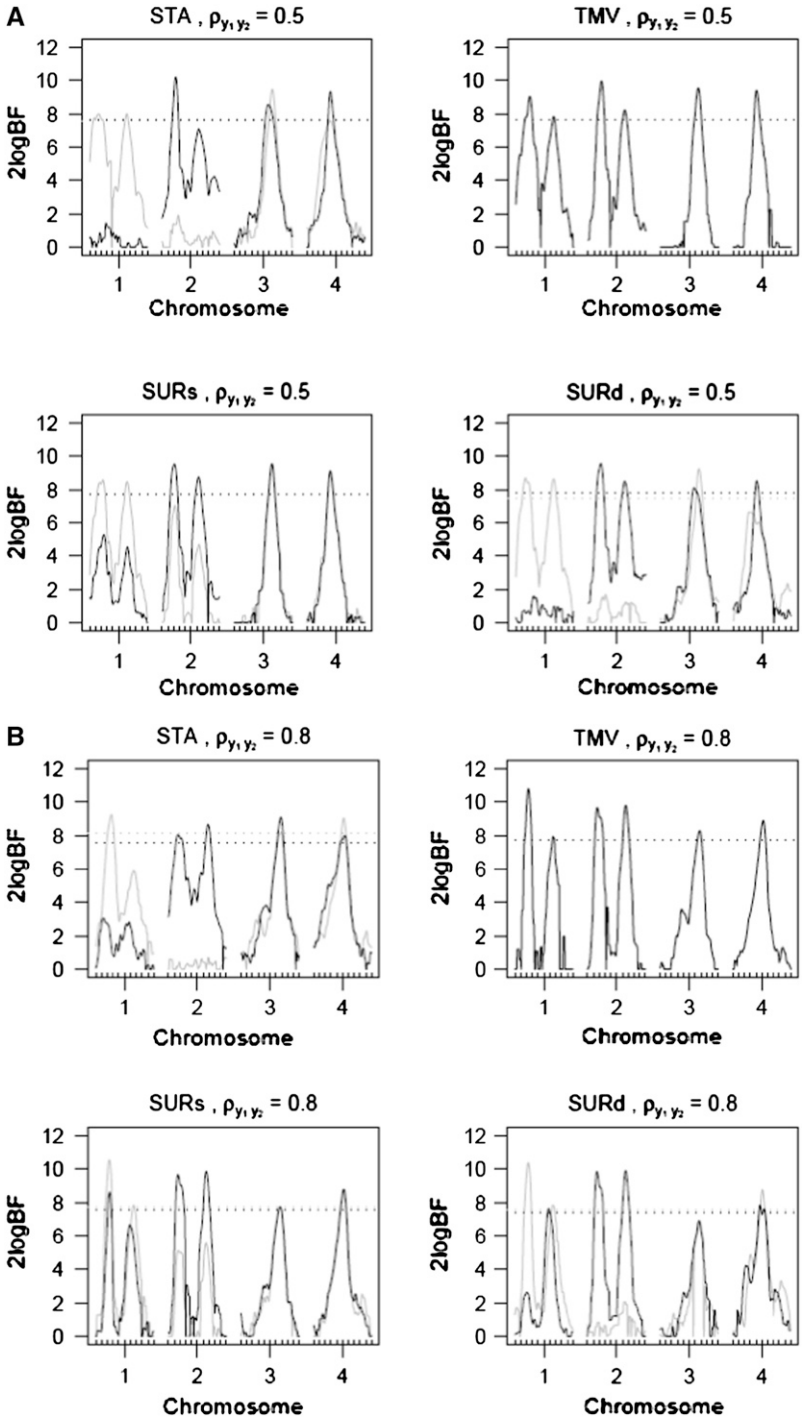

FIGURE 2.—(A) 2 logBF profile for $n = 200$ and $\rho_{y_1 y_2} = 0.5$ for all four methods. Shaded curves represent 2 logBF profile for y_1 and solid curves that for y_2; the shaded dotted line denotes the 95% threshold for y_1 for the null model and the solid dotted lines denote the same for y_2. On the *x*-axis, large tick marks represent chromosomes and small tick marks represent markers. (B) 2 logBF profile for $n = 200$ and $\rho_{y_1 y_2} = 0.8$ for all four methods. Shaded curves represent 2 logBF profile for y_1 and solid curves that for y_2; shaded dotted lines denote the 95% threshold for y_1 for the null model and solid dotted lines denote the same for y_2. On the *x*-axis, large tick marks represent chromosomes and small tick marks represent markers.

R/qtlbim provides tools to monitor mixing behavior and convergence of the simulated Markov chain, either by examining trace plots of the sample values of scalar quantities of interest, such as the numbers of QTL and main effects, or by using formal diagnostic methods provided in the package R/coda. R/qtlbim provides extensive informative graphical and numerical summaries of the MCMC output to infer and interpret the genetic architecture of complex traits (YANDELL *et al.* 2007).

SIMULATION STUDIES

Design and method: With an increased complexity and sophistication of a proposed method, it is very important to compare its performance with existing methods in an objective way. To achieve this end, we conduct extensive simulation studies to compare the proposed methods for joint analysis of multiple traits among themselves and also with a single trait-by-trait analysis. Any simulation experiment is necessarily in-

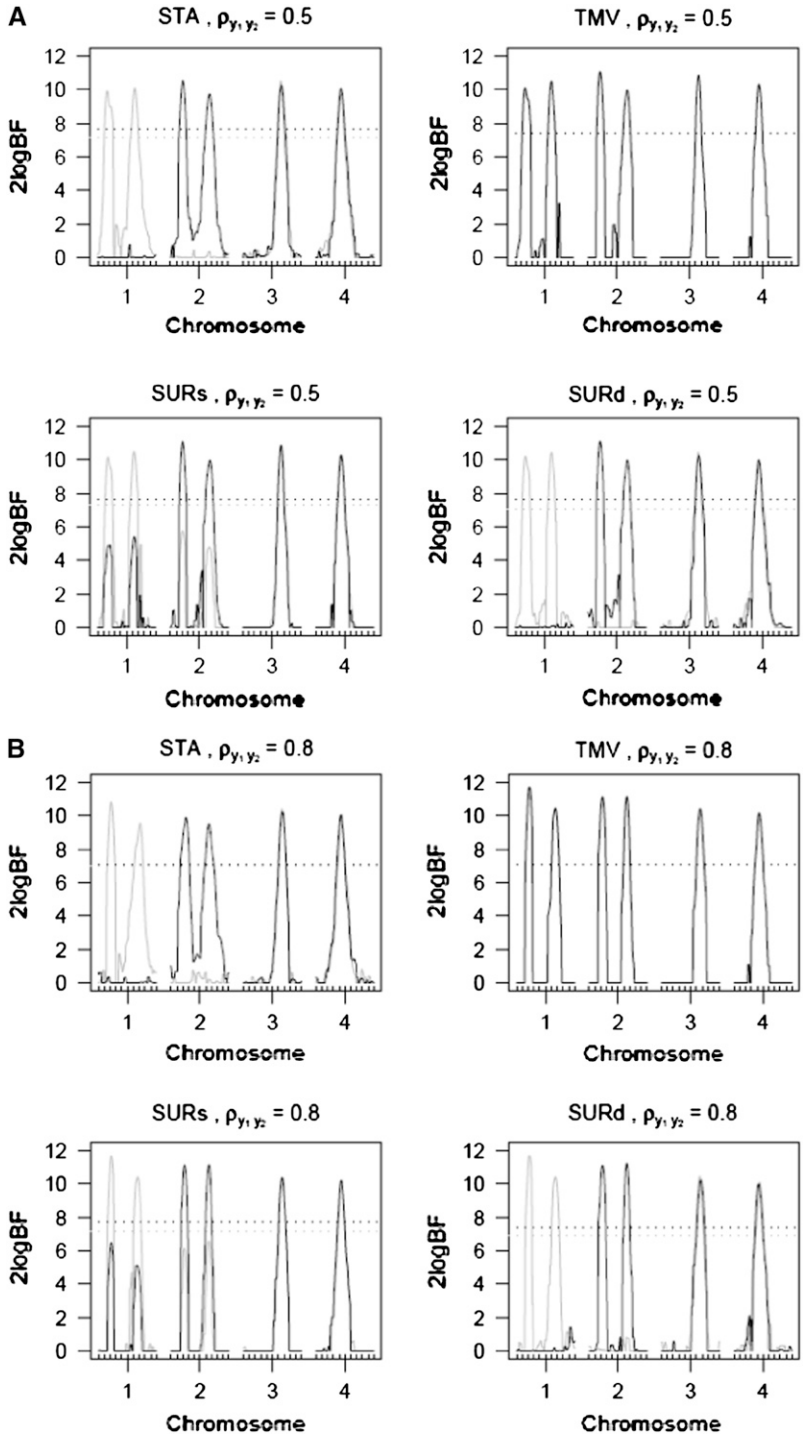

FIGURE 3.—(A) 2 logBF profile for $n = 500$ and $\rho_{y_1 y_2} = 0.5$ for all four methods. Shaded curves represent 2 logBF profile for y_1 and solid curves that for y_2; shaded dotted lines denote the 95% threshold for y_1 for the null model and solid dotted lines denote the same for y_2. On the *x*-axis, large tick marks represent chromosomes and small tick marks represent markers. (B) 2 logBF profile for $n = 500$ and $\rho_{y_1 y_2} = 0.8$ for all four methods. Shaded curves represent the 2 logBF profile for y_1 and solid curves that for y_2; shaded dotted lines denote the 95% threshold for y_1 for the null model and solid dotted lines denote the same for y_2. On the *x*-axis, large tick marks represent chromosomes and small tick marks represent markers.

complete and does not represent real QTL experiments. Nevertheless, we try to simulate a relatively "realistic" QTL model and evaluate the performance with different sample sizes and correlation structures.

We consider a backcross population with sample sizes of 100, 200, and 500 to represent very small, small, and large sample sizes. Two continuous traits (y_1 and y_2) are considered for simplicity. We simulate a genome with 19 chromosomes, each of length 100 cM with 11 equally spaced markers (markers placed 10 cM apart) on each chromosome. Ten percent of the genotypes of these markers were assumed to be randomly missing in all cases. For each of the three sample sizes, we consider two correlation structures, namely, low and high with $\rho_{y_1 y_2} = 0.5$ and $\rho_{y_1 y_2} = 0.8$. Therefore, we have six cases with three samples sizes and two correlation structures. For each of these six cases, we simulate six QTL (Q_1–Q_6) that control the phenotypes: Q_1 and Q_2 (Q_3 and Q_4) are nonpleitropic QTL, influencing only the trait y_1 (y_2) with moderate-sized and weak effects, respectively; Q_5 is a moderate-sized pleiotropic QTL affecting both y_1 and y_2; while Q_6 is a weak pleiotropic QTL affecting both y_1

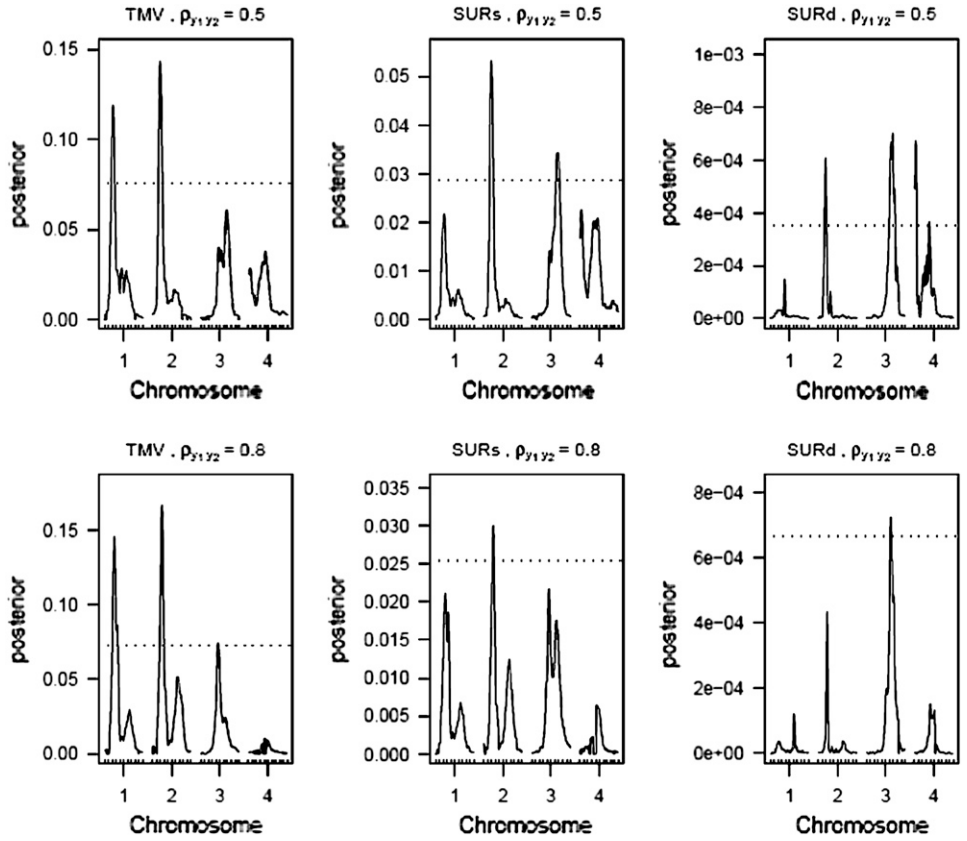

FIGURE 4.—Profile of posterior inclusion probabilities for the test of pleiotropy for $n = 100$. The dotted line represents the 95% threshold for the null model. On the x-axis, large tick marks represent chromosomes and small tick marks represent markers.

and y_2. Table 1 presents the simulated positions of six QTL, their effect values, and their heritabilities (proportion of the phenotypic variation explained by a QTL).

For each of the six cases, we generate 100 replicated data sets, resulting in 600 total data sets. For each of these 600 data sets we perform analysis using four methods, namely, the STA, joint analysis using a TMV model, joint analysis using a SURd model, and joint analysis using a SURs model. For all analyses, pseudomarkers were placed every 1 cM across the entire genome, resulting in a total of 1919 possible QTL positions. The prior expected number of main-effect QTL was set at $l_0 = 4$, and the upper bound on the number of QTL was then $L = 10$ ($= l_0 + 3\sqrt{l_0}$, also see YI *et al.* 2005). To check posterior sensitivity to these prespecified values, we analyzed the data with several other values of l_0 and L and obtained essentially identical results. We ran the MCMC algorithm for 12×10^4 times after discarding the first 1000 iterations as burn-in. The chain was thinned by considering one in every 40 samples, rendering 3000 samples from the joint posterior distribution. The saved posterior samples were used to make inference about the genetic architecture.

To illustrate the advantages of using a more complex method of analysis it is important to have an objective and reproducible plan of evaluation. However, in the model selection framework of multiple QTL mapping this assessment becomes a little more complicated as one has to account for model uncertainty (BURNHAM and ANDERSON 2002). The model selection uncertainty can lead to underestimation about the quantities of interest, which could be quite large as shown by MILLER (1984) in the regression context. One could use the Jeffreys relative scaling of Bayes factors to assess strength of evidence, but the behavior of Bayes factors in complex situations like multiple-QTL mapping is unknown. Nonetheless, to assess the performance of different methods we adopt a simple approach. For all six cases we simulate 100 null (no-QTL) data sets and compute the genomewide maximum 2 $\log_e$BF (twice the natural logarithm of Bayes factors) for each trait. The 95th percentile of the max 2 $\log_e$BF empirical distribution is considered as the threshold value above which a QTL would be deemed "significant." At each replication, the number of correctly identified QTL and the number of incorrectly identified or extraneous QTL are recorded. A peak in the 2 logBF profile is considered a QTL if it crosses the significance threshold. It is deemed correct if it is within 10 cM (BROMAN and SPEED 2002) of a true QTL. If there is more than one peak within 10 cM of the true QTL, only one is considered correct.

Results: Table 2 represents the average correct and extraneous (incorrect) QTL detections for the six situations and for all four methods for y_1 and y_2, respectively. It can be seen that TMV detects the highest number of correct as well as the highest number of extraneous QTL. All the multivariate methods detect the higher number of correct QTL compared to the univariate

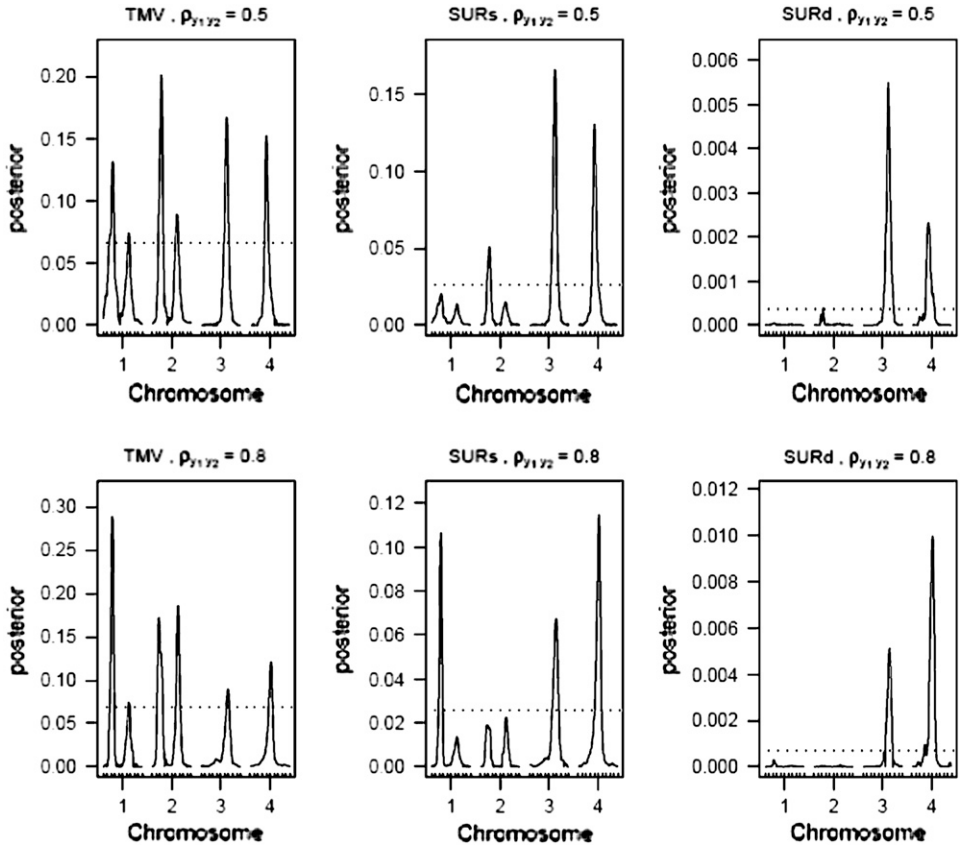

FIGURE 5.—Profile of posterior inclusion probabilities for the test of pleiotropy for $n = 200$. The dotted line represents the 95% threshold for the null model. On the *x*-axis, large tick marks represent chromosomes and small tick marks represent markers.

procedure (especially in high correlation cases). The performance of both the QTL SUR models is very close.

Figures 1–3 display the 2 $\log_e$BF profile for chromosomes 1–4 for the three sample sizes ($n = 100, 200, 500$), respectively, in the four frameworks, namely, SURs, SURd, TMV, and STA. Chromosomes 5–19 had negligible QTL samples (not shown). As can be seen in Figure 1A, both SUR procedures barely detected the moderate effects Q_1 and Q_3 in the low correlation case, but strongly detected the same QTL in the high correlation case (Figure 1B); STA could barely detect them in either case; TMV incorrectly detected Q_1 and Q_3 for both traits. Figure 2, A and B, shows SURd performed reasonably well in detecting all six QTL for both high and low levels of correlation between traits; SURs performed similarly but detected Q_1 for both traits incorrectly; however, STA failed to detect the weak effects Q_2 (Q_4) in the high (low) correlation cases; TMV identified all six QTL for each trait but only four QTL were true for each trait. Finally, Figure 3, A and B, shows STA, SURs, and SURd could correctly identify all six QTL clearing the threshold for both correlation situations comfortably; TMV, however, strongly detected all six QTL for each trait, as in Figure 2, A and B.

Figures 4–6 display the posterior probability profiles for the three sample sizes for testing pleiotropy (a certain locus is simultaneously included in the model for both traits) in the TMV, SURs, and SURd frameworks. We follow the same procedure to measure the threshold values for pleiotropic posterior probabilities. As can be seen in Figure 4, TMV incorrectly detected Q_1 and Q_3 as pleiotropic QTL in the low correlation case; but in the high correlation case it could only feebly detect the true moderate pleiotropic QTL (Q_5) in addition to the incorrectly detected ones; SURs detected Q_5 correctly and Q_3 incorrectly in both correlation structures; SURd incorrectly detected Q_3 in the low correlation case, but correctly detected both pleiotropic QTL (Q_5 and Q_6) in the high correlation case. In Figures 4 and 6, TMV incorrectly detected all 6 QTL as pleiotropic QTL in both correlation structures. In Figures 5 and 6, SURs detected both pleiotropic QTL correctly but also detected some extraneous nonpleiotropic QTL for both correlation structures. SURd, however, detected both pleiotropic QTL correctly without any incorrect detection in the small and large sample size situations for both correlation structures.

The average times taken to conduct each MCMC for all six cases and four methods are presented in Table 3. TMV was the fastest in all cases followed by SURs, STA, and SURd. However, the maximum difference between the fastest and the slowest was only 1.62 min (1 min 37 sec). So computationally complexity does not really pose a great threat.

In conclusion, it is evident and expected that the multivariate procedures outperform STA in the small sample size and high correlation situations. However, one should not use the traditional multivariate model

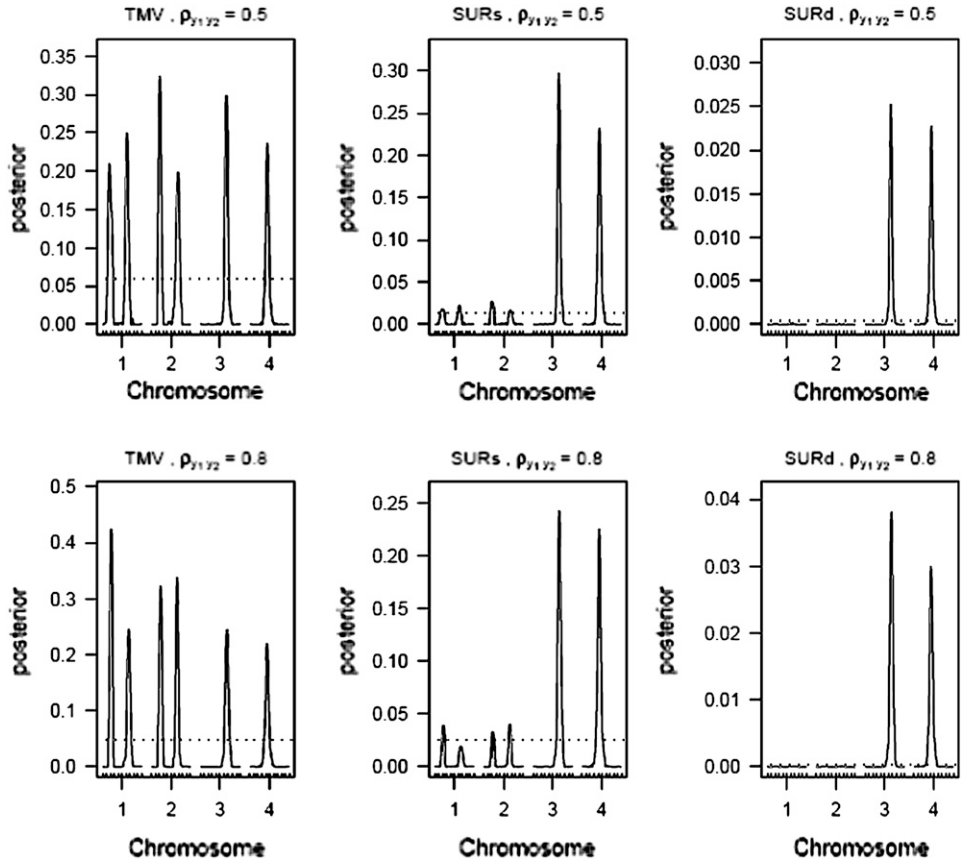

FIGURE 6.—Profile of posterior inclusion probabilities for the test of pleiotropy for $n = 500$. The dotted line represents the 95% threshold for the null model. On the x-axis, large tick marks represent chromosomes and small tick marks represent markers.

to detect nonpleiotropic QTL as there was astounding evidence of it being prone to erroneous detection. Both the SUR models performed well, but SURs provided slightly false evidence for a QTL influencing y_1 (say) for y_2. If one wants to detect only pleiotropic QTL, a traditional multivariate model can be used, but, in any other situations, a SURd procedure is recommended in light of a marginal increase in computational time.

DISCUSSION

Our goal in this article was to develop a comprehensive genomewide QTL mapping technique for multiple traits and assess its performance with existing single-trait analysis. When a QTL mapping experiment is conducted, an experimenter rarely measures only a single trait. However, even in the presence of data on more than one trait, there has been a lack of joint analysis of all traits primarily due to the lack of a comprehensive multivariate multiple-QTL mapping technique. From the simulation experiments we have observed that for relatively highly correlated traits the performance of multivariate methods is better compared to single-trait analysis in terms of QTL identification.

We have proposed two separate models for the joint analysis of multiple traits, namely, the seemingly unrelated regression and the traditional multivariate model. The advantage of the SUR model is that it permits all traits to have separate genetic models, much like an independent trait-by-trait analysis but including the correlation structure between the traits, thereby making it more powerful and precise. The traditional multivariate model, however, assumes the same genetic model for all traits. In the situation that we considered in the simulation experiment, we saw poor performance of the traditional multivariate model in terms of accuracy and extraneous detections. The traditional multivariate model is appropriate in the extreme sense when all detectable QTL are pleiotropic (influencing all traits simultaneously). Rarely, knowledge of this magnitude about a complex trait is known *a priori*. In general, we recommend using a SUR model.

We investigated two different QTL SUR models, namely, SURs and SURd. The performance of both

TABLE 3

Average MCMC time (in minutes) for four methods

$(n, \rho_{y_1y_2})$	STA	TMV	SURs	SURd
(100, 0.5)	1.17	0.96	1.10	1.18
(100, 0.8)	1.18	0.98	1.09	1.16
(200, 0.5)	2.47	1.99	2.23	2.52
(200, 0.8)	2.48	2.06	2.22	2.45
(500, 0.5)	6.94	6.14	6.51	7.76
(500, 0.8)	6.92	6.11	6.45	7.51

these QTL SUR models has been good. SURs can favor, though very slightly, a QTL of no effect on one trait but having large effect on another trait. In these situations SURd is recommended, since it consistently inferred the correct underlying genetic architecture in simulations. However, the current sampling scheme for updating the genotypes of pleiotropic QTL based on SURd may be suboptimal (as indicated by one of the reviewers), because we always treat the genotypes for different traits separately. In the case where inferring genotypes is difficult we would advocate the use of SURs or replace the genotypes by their conditional expectation in our QTL SUR models (*i.e.*, similar to Haley–Knott regression in QTL analysis). We also can improve the step of updating the genotypes of pleiotropic QTL by using a joint sampling method.

We have adopted the composite model space approach (Yi 2004) and extended it to the multivariate case. The advantage of this approach is that it provides a very efficient way to walk through the space of models, spending more time at "good" models. The key idea behind this approach is to reduce a variable dimensional problem (number of unknown QTL) to a fixed dimensional space and impose a constraint on the maximum number of QTL that can be detected. Our MCMC algorithm has smart strategies to improve efficiency and conduct genomewide scans quickly. For example, we developed a novel one-at-a-time Gibbs sampler to sample regression coefficients that allows us to avoid inverting matrices, saving a lot of precious computational time. In high dimensional problems, inverting extremely large matrices for typically >100,000 iterations can be very computationally taxing and prohibits the use of a multivariate algorithm (as seen in the implementation of Verzilli *et al.* 2005). We also use the inverse of the variance–covariance matrix for the same reason. We have used informative hierarchical priors for the regression coefficients that typically reflect most QTL mapping situations.

We have developed SUR models for QTL that act in a strictly additive manner. However, it is important to mention that this might not be a good assumption especially in light of the growing number of QTL studies providing evidence in favor of interactions between QTL. Our method can extend to include gene–gene and gene–environment interactions in a natural way. In the presence of such interactions, the search space for possible QTL increases dramatically. We plan to investigate the performance of epistatic SUR methods in the future. We also plan to extend the multivariate framework to a mixture of continuous, binary, and ordinal traits.

We thank the reviewers for their helpful comments on the previous version of this manuscript. This work was supported by the following National Institutes of Health grants: R01 GM069430 (N.Y. and B.Y.), National Institute of Diabetes and Digestive and Kidney Diseases (NIDDK) 5803701 (B.Y.), NIDDK 66369-01 (B.Y.), and National Institute of General Medical Sciences/R01 PA-02-110 (B.Y.).

LITERATURE CITED

Ball, R. D., 2001 Bayesian methods for quantitative trait loci mapping based on model selection: approximate analysis using the Bayesian information criterion. Genetics **159:** 1351–1364.

Broman, K. W., and T. Speed, 2002 A model selection approach for the identification of quantitative trait loci in experimental crosses. J. R. Stat. Soc. B **64**(4): 641–656.

Broman, K. W., H. Wu, Ś. Sen and G. A. Churchill, 2003 R/qtl: QTL mapping in experimental crosses. Bioinformatics **19:** 889–890.

Burnham, K. P., and D. R. Anderson, 2002 *Model Selection and Multimodel Inference.* Springer-Verlag, New York.

Gelman, A., J. Carlin, H. Stern and D. Rubin, 2004 *Bayesian Data Analysis.* Chapman & Hall/CRC, London.

Gilbert, H., and P. Le Roy, 2003 Comparison of three multitrait methods for QTL detection. Genet. Sel. Evol. **35:** 281–304.

Gilbert, H., and P. Le Roy, 2004 Power of three multitrait methods for QTL detection in crossbreed populations. Genet Sel. Evol. **36:** 347–361.

Griffiths, W. E., 2001 *Bayesian Inference in the Seemingly Unrelated Regressions Model* (Working Series Paper 793). Department of Economics, University of Melbourne, Melbourne, Australia.

Hackett, C. A., R. C. Meyer and W. T. B. Thomas, 2001 Multi-trait QTL mapping in barley using multivariate regression. Genet. Res. Camb. **77:** 95–106.

Huang, J., and Y. Jiang, 2003 Genetic linkage analysis of a dichotomous trait incorporating a tightly linked quantitative trait in affected sib pairs. Am. J. Hum. Genet. **72:** 949–960.

Jackson, A. U., A. Fornés, A. Galecki, R. A. Miller and D. T. Burke, 1999 Multiple-trait quantitative trait loci analysis using a large mouse sibship. Genetics **151:** 785–795.

Jiang, C., and Z.-B. Zeng, 1995 Multiple trait analysis of genetic mapping for quantitative trait loci. Genetics **140:** 1111–1127.

Jiang, C., and Z.-B. Zeng, 1997 Mapping quantitative trait loci with dominant and missing markers in various crosses from two inbred lines. Genetica **101:** 47–58.

Kao, C.-H., and Z.-B. Zeng, 2002 Modeling epistasis of quantitative trait loci using Cockerham's model. Genetics **160:** 1243–1261.

Knott, S. A., and C. S. Haley, 2000 Multitrait least squares for quantitative trait loci detection. Genetics **156:** 899–911.

Lander, E. S., and D. Botstein, 1989 Mapping Mendelian factors underlying quantitative traits using RFLP linkage maps. Genetics **121:** 185–199.

Lange, C., and J. C. Whittaker, 2001 Mapping quantitative trait loci using generalized estimating equations. Genetics **159:** 1325–1337.

Liu, J., Y. Liu, X. Liu and H.-W. Deng, 2007 Bayesian mapping of quantitative trait loci for multiple complex traits with the use of variance components. Am. J. Hum. Genet. **81:** 304–320.

Lund, M. S., P. Sørensen, B. Guldbrandtsen and D. A. Sorensen, 2003 Multitrait fine mapping of quantitative trait loci using combined linkage disequilibria and linkage analysis. Genetics **163:** 405–410.

Mähler, M., C. Most, S. Schmidtke, J. P. Sundberg, R. Li *et al.*, 2002 Genetics of colitis susceptibility in IL-10-deficient mice: backcross versus F2 results contrasted by principal component analysis. Genomics **80:** 274–282.

Mangin, B., P. Thoquet and N. Grimsley, 1998 Pleiotropic QTL analysis. Biometrics **54:** 88–99.

Meuwissen, T. H., and M. E. Goddard, 2004 Mapping multiple QTL using linkage disequilibrium and linkage analysis information and multitrait data. Genet. Sel. Evol. **36:** 261–279.

Miller, A. J., 1984 Selection of subsets of regression variables. J. R. Stat. Soc. A **147:** 389–425.

Plummer, M., N. Best, K. Cowles and K. Vines, 2004 *Output Analysis and Diagnostics for MCMC*, v. 0.9–5. Institute of Mathematical Statistics, Beachwood, OH.

Raftery, A. E., D. Madigan and J. A. Hoeting, 1997 Bayesian model averaging for linear regression models. J. Am. Stat. Assoc. **92:** 179–191.

Satagopan, J. M., and B. S. Yandell, 1996 Estimating the number of quantitative trait loci via model determination. Special Contributed Paper Session on Genetic Analysis of Quantitative Traits and Complex Diseases. Biometric Section, Joint Statistical Meeting, Chicago.

Sen, Ś., and G. A. Churchill, 2001 A statistical framework for quantitative trait mapping. Genetics **159:** 371–387.

Sillanpää, M. J., and J. Corander, 2002 Model choice in gene mapping: what and why. Trends Genet. **18:** 301–307.

Smith, M., and R. Kohn, 2000 Nonparametric seemingly unrelated regression. J. Econometrics **98:** 257–281.

Verzilli, C. J., N. Stallard and J. C. Whittaker, 2005 Bayesian modeling of multivariate quantitative traits using seemingly unrelated regression. Genetic Epidemiol. **28:** 313–325.

Vieira, C., E. G. Pasyukova, Z.-B. Zeng, J. B. Hackett, R. F. Lyman *et al.*, 2000 Genotype-environment interaction for quantitative trait loci affecting life span in *Drosophila melanogaster*. Genetics **154:** 213–227.

Wang, H., Y. C. M. Zhang, X. Li, G. L. Masinde, S. Mohan *et al.*, 2005 Bayesian shrinkage estimation of quantitative trait loci parameters. Genetics **170:** 465–480.

Williams, J. T., H. Begleiter, B. Porjesz, H. J. Edenberg, T. Foroud *et al.*, 1999a Joint multipoint linkage analysis of multivariate qualitative and quantitative traits. II. Alcoholism and event-related potentials. Am. J. Hum. Genet. **65:** 1148–1160.

Williams, J. T., P. Van Eerdewegh, L. Almasy and J. Blangero, 1999b Joint multipoint linkage analysis of multivariate qualitative and quantitative traits. I. Likelihood formulation and simulation results. Am. J. Hum. Genet. **65:** 1134–1147.

Xu, C., Z. Li and S. Xu, 2005 Joint mapping of quantitative trait loci for multiple binary characters. Genetics **169:** 1045–1059.

Yang, R., and S. Xu, 2007 Bayesian shrinkage analysis of quantitative trait loci for dynamic traits. Genetics **176:** 1169–1185.

Yandell, B. S., T. Mehta, S. Banerjee, D. Shriner, R. Venkataraman *et al.*, 2007 R/qtlbim: QTL with Bayesian interval mapping in experimental crosses. Bioinformatics **23**(5): 641–643.

Yi, N., 2004 A unified Markov chain Monte Carlo framework for mapping multiple quantitative trait loci. Genetics **167:** 967–975.

Yi, N., and D. Shriner, 2008 Advances in Bayesian multiple QTL mapping in experimental designs. Heredity **100:** 240–252.

Yi, N., and S. Xu, 2002 Mapping quantitative trait loci with epistatic effects. Genet. Res. Camb. **79:** 185–198.

Yi, N., S. Xu and D. B. Allison, 2003 Bayesian model choice and search strategies for mapping interacting quantitative trait loci. Genetics **165:** 867–883.

Yi, N., B. S. Yandell, G. A. Churchill, D. B. Allison, E. J. Eisen *et al.*, 2005 Bayesian model selection for genomewide epistatic quantitative trait loci analysis. Genetics **170:** 1333–1344.

Yi, N., D. Shriner, S. Banerjee, T. Mehta, D. Pomp *et al.*, 2007 An efficient Bayesian model selection approach for interacting QTL models with many effects. Genetics **176:** 1865–1877.

Zellner, A., 1962 An efficient method of estimating seemingly unrelated regressions and tests for aggregation bias. J. Am. Stat. Assoc. **57:** 348–368.

Zeng, Z.-B., T. Wang and W. Zou, 2005 Modeling quantitative trait loci and interpretation of models. Genetics **169:** 1711–1725.

Communicating editor: J. B. Walsh

APPENDIX A: PRIOR DISTRIBUTIONS

The independent priors across traits are straightforward extensions of Yi *et al.* (2005, 2007). We describe the priors on $(\boldsymbol{\lambda}_t, \boldsymbol{\gamma}_t, \mu_t, \boldsymbol{\beta}_t)$ for each trait, highlighting the distinctions pertinent to multiple correlated traits.

The prior distribution on QTL locations is uniformly distributed over the preset loci across the genome (Yi *et al.* 2005). Two constraints can be incorporated into the prior on QTL locations to reduce the model space: the first restricts the spacing among multiple linked QTL and the second restricts the number of detectable QTL on each chromosome (see Yi *et al.* 2007).

For the vector of indicators $\boldsymbol{\gamma}_t$, we could use an independence prior, $p(\boldsymbol{\gamma}_t) = \prod_j w_t^{\gamma_{tj}}(1-w_t)^{1-\gamma_{tj}}$, with w_t being the prior inclusion probability of each effect for the tth trait. A useful reduction can be achieved by setting $w_1 = \cdots = w_T$. To specify w_t, we first determine the prior expected numbers of main-effect QTL and then solve for w_t from the expressions of the prior expected numbers (see Yi *et al.* 2005). The prior expected number of main-effect QTL could be set to the number of QTL detected by traditional mapping methods.

The prior for the overall mean μ_t is chosen to be normally distributed with mean and variance being sample mean and variance of the tth trait, respectively. For the genetic effects $\boldsymbol{\beta}_t$, we extend the prior of Yi *et al.* (2007) that assumes that different types of effects (*e.g.*, additive effects or dominance effects) follow different prior distributions. For type k, effects β_{tj}^k have the prior, $\beta_{tj}^k \mid \gamma_{tj} \sim (1-\gamma_{tj})I_0 + \gamma_{tj}N(0, \sigma_{tk}^2)$, where γ_{tj} is the indicator variable for β_{tj}^k, and I_0 is a point mass at 0. Under this prior, when $\gamma_{tj} = 0$, β_{tj}^k is assigned to be 0 and thus is actually removed from the model; when $\gamma_{kj} = 1$, β_{tj}^k follows a normal distribution $N(0, \sigma_{tk}^2)$. The variance σ_{tk}^2 is treated as a random variable with an inverse-χ^2 hyperprior distribution; *i.e.*, $\sigma_{tk}^2 \sim$ Inv-$\chi^2(\nu_{tk}, s_{tk}^2)$. The degrees of freedom ν_{tk} control the skewness of the prior for σ_{tk}^2, with larger values recommended (here $\nu_{tk} = 6$) to tightly center the prior around s_{tk}^2 (see Yi *et al.* 2007). The scale parameter s_{tk}^2 controls the prior proportion of phenotypic variance explained by β_{tj}^k. We set $s_{tk}^2 = (\nu_{tk}-2)hV_t/(\nu_{tk}V_{tj}^k)$, leading to the proportion of phenotypic variance explained by β_{tj}^k being h, where V_t is the phenotypic variance of trait t, and V_{tj}^k is the sample variance for the column of $\mathbf{X}$ associated with effect β_{tj}^k. Expected effect heritability, h, can be set small (say 0.05–0.2) to reflect prior knowledge about genetic architecture.

APPENDIX B: CONDITIONAL POSTERIOR DISTRIBUTIONS

We here derive conditional posterior distribution for each unknown from the joint posterior distribution (3). Denote all the unknowns by $\boldsymbol{\theta}$; *i.e.*, $\boldsymbol{\theta} = (\boldsymbol{\mu}, \boldsymbol{\beta}, \boldsymbol{\sigma}, \boldsymbol{\Sigma}^{-1}, \mathbf{g}, \boldsymbol{\lambda}, \boldsymbol{\gamma})$. We first present the conditional posterior distributions for the model SURd and then make some changes to the models SURs and TMV if necessary.

Conditional posterior distribution of each μ_t: The conditional posterior distribution for the overall mean of the tth trait, μ_t, can be shown to be

$$\mu_t \mid \boldsymbol{\theta}_-, \mathbf{y} \sim N\left(\frac{\sum_{i=1}^{n}(y_i - \boldsymbol{\mu}_{-t} - \mathbf{X}_i\boldsymbol{\beta})\Sigma_{\cdot t}^{-1}}{n\Sigma_{tt}^{-1}}, \frac{1}{n\Sigma_{tt}^{-1}}\right), \tag{B1}$$

where $\boldsymbol{\theta}_-$ represents all elements of $\boldsymbol{\theta}$ except μ_t, $\boldsymbol{\mu}_{-t}$ is the vector $\boldsymbol{\mu}$ with the tth element μ_t replaced by 0, $\Sigma_{\cdot t}^{-1}$ is the tth column of $\boldsymbol{\Sigma}^{-1}$, and Σ_{tt}^{-t} is the (t, t) element of $\boldsymbol{\Sigma}^{-1}$. Since the conditional posterior is a standard distribution, a Gibbs sampler can be easily performed.

Conditional posterior distribution of each β_{tj}: If the jth effect of the tth trait, β_{tj}, is included in the model, the conditional posterior distribution of β_{tj} can be shown to be

$$\beta_{tj} \mid \boldsymbol{\theta}_-, \mathbf{y} \sim N\left(\frac{\sum_{i=1}^{n} x_{tij}(y_i - \boldsymbol{\mu} - \mathbf{X}_i\boldsymbol{\beta}_{-tj})\Sigma_{\cdot t}^{-1}}{\Sigma_{tt}^{-1}\sum_{i=1}^{n} x_{tij}^2 + \sigma_{tj}^{-2}}, \frac{1}{\Sigma_{tt}^{-1}\sum_{i=1}^{n} x_{tij}^2 + \sigma_{tj}^{-2}}\right), \tag{B2}$$

where $\boldsymbol{\theta}_-$ represents all elements of $\boldsymbol{\theta}$ except β_{tj}, $\boldsymbol{\beta}_{-tj}$ is the vector $\boldsymbol{\beta}$ with the element β_{tj} replaced by 0, $\Sigma_{\cdot t}^{-1}$ and Σ_{tt}^{-t} are defined as in (A1), and x_{tij} is the main-effect contrast for the jth effect for the tth trait and the ith individual. Note that $x_{tij} = x_{ij} \forall t$ for SURs and TMV.

Conditional posterior distribution of each σ_{tk}^2: For each type of genetic effects (additive and dominance), the conditional posterior distribution of σ_{tk}^2 is an inverse-χ^2 distribution,

$$\sigma_{tk}^2 \mid \boldsymbol{\theta}_-, \mathbf{y} \sim \text{Inv-}\chi^2\left(\nu_{tk} + q_{tk}, \frac{\nu_{tk}s_{tk}^2 + \sum_j(\beta_{tj}^k)^2}{\nu_{tk} + q_{tk}}\right), \tag{B3}$$

where q_{tk} is the number of nonzero effects in $\{\beta_{tj}^k; j = 1, 2, \cdots\}$, and other parameters are defined earlier.

Conditional posterior distribution of $\boldsymbol{\Sigma}^{-1}$: Keeping the computationally efficient goal in mind, it should be noted that generating $\boldsymbol{\Sigma}$ would involve computing its inverse to draw samples from (B1) and (B2) in each iteration. So, it is not only convenient to work with $\boldsymbol{\Sigma}^{-1}$ but computationally efficient as well. The conditional posterior distribution for $\boldsymbol{\Sigma}^{-1}$ can be calculated

$$\boldsymbol{\Sigma}^{-1} \mid \boldsymbol{\theta}_-, \mathbf{y} \sim |\boldsymbol{\Sigma}^{-1}|^{(1/2)(n-T-1)} \exp\left\{-\frac{1}{2}tr(\boldsymbol{\Omega}\boldsymbol{\Sigma}^{-1})\right\} = \text{Wishart}_T(\boldsymbol{\Omega}^{-1}, n), \tag{B4}$$

where $\boldsymbol{\theta}_-$ represents all elements of $\boldsymbol{\theta}$ except $\boldsymbol{\Sigma}^{-1}$, and $\boldsymbol{\Omega}$ is a $T \times T$ matrix of residuals where the (t, t')th element of $\boldsymbol{\Omega}$, $\omega_{tt'} = \sum_{i=1}^{n}\left(y_{ti} - \hat{\mu}_t - \sum_j \hat{\beta}_{tij}x_{tij}\right)\left(y_{t'i} - \hat{\mu}_{t'} - \sum_j \hat{\beta}_{t'ij}x_{t'ij}\right)$. Since the posterior of $\boldsymbol{\Sigma}^{-1}$ follows a standard Wishart distribution, a Gibbs sampler can be used to generate samples. An alternative Metropolis algorithm could also be used to generate samples where a newly generated iterate $\boldsymbol{\Sigma}_{\text{new}}^{-1}$ is accepted over an old value $\boldsymbol{\Sigma}_{\text{old}}^{-1}$ with probability

$$\alpha = \min\left\{1, \frac{p(\boldsymbol{\Sigma}_{\text{new}}^{-1} \mid \boldsymbol{\theta}_-, \mathbf{y})q(\boldsymbol{\Sigma}_{\text{old}}^{-1})}{p(\boldsymbol{\Sigma}_{\text{old}}^{-1} \mid \boldsymbol{\theta}_-, \mathbf{y})q(\boldsymbol{\Sigma}_{\text{new}}^{-1})}\right\} = \min\left\{1, \frac{|\boldsymbol{\Sigma}_{\text{new}}^{-1}|^{n/2}\exp\{-(1/2)tr(\boldsymbol{\Omega}\boldsymbol{\Sigma}_{\text{old}}^{-1})\}}{|\boldsymbol{\Sigma}_{\text{old}}^{-1}|^{n/2}\exp\{-(1/2)tr(\boldsymbol{\Omega}\boldsymbol{\Sigma}_{\text{new}}^{-1})\}}\right\}, \tag{B5}$$

where $q(.)$ is the proposal density that is assumed to be the same as its prior. We have implemented both the Gibbs sampler and the Metropolis algorithm for updating $\boldsymbol{\Sigma}^{-1}$ and in either case we get similar results.

Conditional posterior distribution of each g_{tiq}: If locus q for trait t is included in the model and the genotype g_{tiq} of individual i is not observed, the conditional posterior distribution of g_{tiq} is

$$p(g_{tiq} = k \mid \boldsymbol{\theta}_-, \mathbf{y}_i) \propto p(\mathbf{y}_i \mid \boldsymbol{\theta}_-, \mathbf{y}_i, g_{tiq} = k)p(g_{tiq} = k \mid \lambda_{tq}), \tag{B6}$$

where $\boldsymbol{\theta}_-$ represents all elements of $\boldsymbol{\theta}$ except g_{tiq}, $p(\mathbf{y}_i \mid \boldsymbol{\theta}_-, \mathbf{y}_i, g_{tiq} = k)$ is the likelihood for individual i calculated by model (2), and $p(g_{tiq} = k \mid \lambda_q)$ is the prior probability of $g_{tiq} = k$. This posterior is a simple multinomial distribution and thus can be sampled directly. If locus q is excluded from the model or g_{tiq} is observed (*e.g.*, for fully observed markers), we do not need to sample g_{tiq}.

Conditional posterior distribution of $\boldsymbol{\lambda}$: If locus q for trait t is included in the model, the joint conditional posterior distribution of the position λ_{tq} and the genotypes $\mathbf{g}_{tq} = (g_{t1q}, \cdots, g_{tnq})$ is

$$p(\lambda_{tq}, \mathbf{g}_{tq} \mid \boldsymbol{\theta}_-, \mathbf{y}) \propto p(\mathbf{y} \mid \boldsymbol{\theta}_-, \lambda_{tq}, \mathbf{g}_{tq})p(\lambda_{tq})p(\mathbf{g}_{tq} \mid \lambda_{tq}), \tag{B7}$$

where $\boldsymbol{\theta}_-$ represents all elements of $\boldsymbol{\theta}$ except λ_{tq} and $\mathbf{g}_{tq}$, $p(\mathbf{y} \mid \boldsymbol{\theta}_-, \lambda_{tq}, \mathbf{g}_{tq})$ is the likelihood calculated by model (2), $p(\lambda_{tq})$ is the prior of λ_{tq}, and $p(\mathbf{g}_{tq} \mid \lambda_{tq}) = \prod_{i=1}^{n} p(\mathbf{g}_{tiq} \mid \lambda_{tq})$ is the prior probability of $\mathbf{g}_{tq}$.

This posterior is not a standard distribution, and thus a Metropolis algorithm is needed to update λ_{tq} and $\mathbf{g}_{tq}$ jointly. We first propose a new position λ^*_{tq} from a proposal distribution $q(\lambda^*_{tq}; \lambda_{tq})$ and then generate new genotypes, g^*_{tiq}, at this new position for all individuals from the conditional posterior (B6). The proposals for λ^*_{tq} and $\mathbf{g}^*_{tq}$ are then accepted simultaneously with probability

$$\alpha = \min\left(1, \frac{p(\lambda^*_{tq}, \mathbf{g}^*_{tq} \mid \boldsymbol{\theta}_-, \mathbf{y}) q(\lambda_{tq}; \lambda^*_{tq}) q(\mathbf{g}_{tq})}{p(\lambda_{tq}, \mathbf{g}_{tq} \mid \boldsymbol{\theta}_-, \mathbf{y}) q(\lambda^*_{tq}; \lambda_{tq}) q(\mathbf{g}^*_{tq})}\right). \tag{B8}$$

The proposal distribution for the new position $q(\lambda^*_q; \lambda_q)$ is usually constructed as uniformly distributed over $2d$ most flanking loci of λ_q, with d being a predetermined tuning integer. In our implementation, we take $d = 2$ and incorporate the preset constraints on QTL positions into our algorithm.

Conditional posterior distribution of each γ_{tj}: The conditional posterior distribution of γ_{tj} can be expressed as

$$p(\gamma_{tj} = 1 \mid \boldsymbol{\theta}_-, \mathbf{y}) = \frac{p(\gamma_{tj} = 1) p(\mathbf{y} \mid \boldsymbol{\theta}_-, \gamma_{tj} = 1)}{p(\gamma_{tj} = 0) p(\mathbf{y} \mid \boldsymbol{\theta}_-, \gamma_{tj} = 0) + p(\gamma_{tj} = 1) p(\mathbf{y} \mid \boldsymbol{\theta}_-, \gamma_{tj} = 1)}, \tag{B9}$$

where $\boldsymbol{\theta}_-$ represents all elements of $\boldsymbol{\theta}$ except γ_{tj} and β_{tj}, $p(\mathbf{y} \mid \boldsymbol{\theta}_-, \gamma_{tj} = 0)$ is calculated using model (2) with β_{tj} replaced by 0, and $p(\mathbf{y} \mid \boldsymbol{\theta}_-, \gamma_{tj} = 1)$ does not depend on β_{tj} and can be calculated using the identity of simple conditional probability

$$p(\mathbf{y} \mid \boldsymbol{\theta}_-, \gamma_{tj} = 1) = \frac{p(\mathbf{y} \mid \boldsymbol{\theta}_-, \gamma_{tj} = 1, \beta_{tj}) p(\beta_{tj})}{p(\beta_{tj} \mid \mathbf{y}, \boldsymbol{\theta}_-, \gamma_{tj} = 1)}, \tag{B10}$$

where $p(\mathbf{y} \mid \boldsymbol{\theta}_-, \gamma_{tj} = 1, \beta_{tj})$ is the phenotype likelihood calculated using model (2), $p(\beta_{tj})$ is the prior distribution of β_{tj}, and $p(\beta_{tj} \mid \mathbf{y}, \boldsymbol{\theta}_-, \gamma_{tj} = 1)$ is the conditional posterior distribution of β_{tj} calculated by (B2). Notationally, the right side of (B10) depends on β_{tj}, but from the definition of $p(\mathbf{y} \mid \boldsymbol{\theta}_-, \gamma_{tj} = 1)$, we know it cannot depend on β_{tj} in a real sense. That is, the factors that depend on β_{tj} in the numerator and the denominator must cancel. Thus, we can compute (B10) by inserting any value of β_{tj} into the expression. A convenient, stable choice is the conditional posterior mean of β_{tj} (Gelman *et al.* 2004; Yi *et al.* 2007).

To calculate the conditional posterior probability (B9), we may need the values of parameters associated with γ_{tj}. If γ_{tj} is currently 0 and the involved QTL(s) is (are) not currently in the model, we first sample new QTL position(s) from their corresponding priors as needed, new genotypes for all individuals, and the prior variance of β_{tj} if this parameter is currently out of the model. If the current value of γ_{tj} is 1, the associated unknowns were already generated at the preceding iteration.

The Gibbs sampler can be used to generate each indicator γ_{tj} from its conditional posterior (B9). However, for the QTL SUR models, using the Gibbs samplers is computationally demanding because the SUR models contain T times the number of indicators as a single-trait model and most of the indicators are zero. To speed up the algorithm we extend the Metropolis–Hastings algorithm proposed by Yi *et al.* (2007) to the QTL SUR models. As with the Gibbs sampler, the MH scheme proceeds to update all indicator variables. Denote the current value of γ_{tj} by C (= 0 or 1). The MH algorithm proposes a new value P (= 0 or 1) for γ_{tj} from the prior probability $p(\gamma_{tj} = C)$. If $P = C$, the MH acceptance probability is 1, and thus γ_{tj} remains at C and there is no need to compute any values. Otherwise, we update γ_{tj} from the current value C to the proposal $1 - C$ with acceptance probability

$$\alpha = \min\left(1, \frac{p(\gamma_{tj} = 1 - C \mid \boldsymbol{\theta}_-, \mathbf{y})}{p(\gamma_{tj} = C \mid \boldsymbol{\theta}_-, \mathbf{y})} \cdot \frac{p(\gamma_{tj} = C)}{p(\gamma_{tj} = 1 - C)}\right), \tag{B11}$$

where $p(\gamma_{tj} = C \mid \boldsymbol{\theta}_-, \mathbf{y})$ and $p(\gamma_{tj} = 1 - C \mid \boldsymbol{\theta}_-, \mathbf{y})$ are calculated in (B9).

The conditional posterior of $\boldsymbol{\gamma}$ for the traditional multivariate model is a little tricky. Since the indicator variable of a particular effect is the same for all traits, the conditional posterior distribution of γ_j can be expressed as

$$p(\gamma_j = 1 \mid \boldsymbol{\theta}_-, \mathbf{y}) = \frac{p(\gamma_j = 1) p(\mathbf{y} \mid \boldsymbol{\theta}_-, \gamma_j = 1)}{p(\gamma_j = 0) p(\mathbf{y} \mid \boldsymbol{\theta}_-, \gamma_j = 0) + p(\gamma_j = 1) p(\mathbf{y} \mid \boldsymbol{\theta}_-, \gamma_j = 1)}, \tag{B12}$$

where γ_j is the indicator variable for the jth effects for all traits, $\boldsymbol{\theta}_-$ represents all elements of $\boldsymbol{\theta}$ except γ_j and β_j, $\underset{\sim}{\beta}_j$ denotes the vector of the jth effects for all traits, and $p(\mathbf{y} \mid \boldsymbol{\theta}_-, \gamma_{tj} = 0)$ is calculated using model (2) with $\underset{\sim}{\beta}_j$ replaced by

0. The integration in (B10) should be with respect to joint distribution of all genetic effects for the traits in question. Proceeding similarly as above we can get

$$p(\mathbf{y} \mid \boldsymbol{\theta}_{-}, \gamma_j = 1) = \frac{p(\mathbf{y} \mid \boldsymbol{\theta}_{-}, \gamma_j = 1, \underset{\sim}{\beta}_j) p(\underset{\sim}{\beta}_j)}{p(\underset{\sim}{\beta}_j \mid \mathbf{y}, \boldsymbol{\theta}_{-}, \gamma_j = 1)}. \tag{B13}$$

As before, a choice of $\underset{\sim}{\beta}_j$ could be the posterior mean of the joint posterior distribution of $\underset{\sim}{\beta}_j$ calculated below,

$$\underset{\sim}{\beta}_j \sim N_T \left(\Sigma_\beta \sum_{i=1}^{n} x_{ij} \boldsymbol{\Sigma}^{-1} (y_{i\cdot} - \boldsymbol{\mu} - \mathbf{x}_{i\cdot}' \underset{\sim}{\beta}_{-j}), \Sigma_\beta \right), \tag{B14}$$

where $x_{i\cdot}$ is the vector of main-effect contrast(s) for the ith individual for all loci, $\Sigma_\beta = \left(\boldsymbol{\Sigma}^{-1} \sum_{i=1}^{n} x_{ij}^2 + \mathrm{diag}(\underset{\sim}{\sigma}_j^{-2}) \right)^{-1}$, $\underset{\sim}{\sigma}_j^2$ is the vector of the variances of the jth genetic effect for all traits, and $\underset{\sim}{\beta}_{-j}$ is the vector of coefficients with β_{tj} ($t = 1, \cdots T$) replaced as 0.